Multiscale and Multiphysics Mechanics, *Vol. 1, No. 1 (2016) 53-64*
DOI: http://dx.doi.org/10.12989/mmm.2016.1.1.053

Nanomechanical behaviors and properties of amyloid fibrils

Bumjoon Choi[1], Sang Woo Lee[1] and Kilho Eom*[2]

[1]*Department of Biomedical Engineering, Yonsei University, Wonju 26493, Republic of Korea*
[2]*Biomechanics Laboratory, College of Sport Science, Sungkyunkwan University, Suwon 16419, Republic of Korea*

(Received April 3, 2015, Revised October 19, 2015, Accepted October 22, 2015)

Abstract. Amyloid fibrils have recently been considered as an interesting material, since they exhibit the excellent mechanical properties such as elastic modulus in the order of 10 GPa, which is larger than that of other protein materials. Despite recent findings of these excellent mechanical properties for amyloid fibrils, it has not been fully understood how these excellent mechanical properties are achieved. In this work, we have studied the nanomechanical deformation behaviors and properties of amyloid fibrils such as their elastic modulus as well as fracture strength, by using atomistic simulations, particularly steered molecular dynamics simulations. Our simulation results suggest the important role of the length of amyloid fibrils in their mechanical properties such that the fracture force of amyloid fibril is increased when the fibril length decreases. This length scale effect is attributed to the rupture mechanisms of hydrogen bonds that sustain the fibril structure. Moreover, we have investigated the effect of boundary condition on the nanomechanical deformation mechanisms of amyloid fibrils. It is found that the fracture force is critically affected by boundary condition. Our study highlights the crucial role of both fibril length and boundary condition in the nanomechanical properties of amyloid fibrils.

Keywords: amyloid fibrils; mechanical deformation mechanisms; molecular dynamics simulation; fracture property; boundary condition

1. Introduction

Amyloid fibrils, which are formed as a one-dimensional nanostructure via protein aggregation (Cherny and Gazit 2008), have been found to play a pivotal role in the pathogenesis of various diseases including neurodegenerative diseases (Pepys 2006, Hamley 2012) and type II diabetes (Hoppener *et al*. 2000). This indicates the necessity of understanding how the fibril structure is formed through self-assembly process, that is, protein aggregation (Straub and Thirumalai 2011). In the last decade, the molecular structure of amyloid fibril has been found to be stabilized through hydrogen bonding between protein chains, which are the aggregation-prone β-strand-rich structural motifs (Cherny and Gazit 2008). As it has recently been revealed that the β-strand-rich structural motif is able to effectively resist a mechanical force (Eom *et al*. 2003, Eom *et al*. 2005, Keten *et al*. 2010), it has been conjectured that amyloid fibril, which is composed of β-sheet-rich structural

*Corresponding author, Professor, Ph.D., E-mail: kilhoeom@skku.edu

http://www.techno-press.org/journals/mmm&subpage=7 ISSN: 2383-7306 (Print), 2456-9711 (Online)

motifs, is able to effectively bear a mechanical force.

In recent years, the nanomechanical properties of amyloid fibrils have been measured based on experiments and computational simulations (Knowles and Buehler 2011). For instance, based on atomic force microscopy (AFM)-based experiments, the nanomechanical properties of amyloid fibrils are measured such that the elastic moduli of the fibrils are found to be in the order of 1 to 10 GPa (Smith *et al*. 2006, Knowles *et al*. 2007), which is comparable to the elastic modulus of a mechanically strong protein material such as spider silk (Gosline *et al*. 1999). A recent experiment based on 4D electron microscopy (Fitzpatrick *et al*. 2013) shows that the vibrational behavior of amyloid fibril due to electron-driven actuation is well dictated by classical elastic beam model such as Euler-Bernoulli beam model, and that the elastic modulus of amyloid fibril is measured in the order of 10 GPa. Buehler and coworkers (Xu *et al*. 2010, Paparcone and Buehler 2011, Solar and Buehler 2012a, 2014) have reported that, based on computational simulations, the nanomechanical properties of amyloid fibrils are critically dependent on their structural features such as the fibril length, and that the strength of the fibrils is determined from the geometrically confined network of hydrogen bonds that sustain the fibril structure. Our previous works (Yoon *et al*. 2011, 2013) report that, based on coarse-grained simulations, the bending elastic modulus of amyloid fibrils is measured in a range of 1 to 10 GPa, which depends on the fibril length. Moreover, our recent simulations (Yoon *et al*. 2014, Choi *et al*. 2015) report that the bending rigidity of amyloid fibrils is estimated in the order of 10^{-26} $N{\cdot}m^2$, and that the fracture toughness of amyloid fibrils is measured as ~30 $kcal{\cdot}mol^{-1}{\cdot}nm^{-3}$, which is comparable to the toughness of a spider silk.

These remarkable nanomechanical properties of amyloid fibrils have received significant attention due to recent findings that these properties are related to the biological functions of amyloid fibrils (Knowles and Buehler 2011). For example, the disruption of cell membrane due to amyloid fibril (Engel *et al*. 2008) may be attributed to the difference between the mechanical properties of amyloid fibril and cell membrane (Fitpatrick *et al*. 2013). Moreover, it has recently been found that the molecular size and fracture strength of prion amyloid fibril are highly correlated with the prion infectivity (Silveira *et al*. 2005, Tanaka *et al*. 2006). Our recent study (Yoon *et al*. 2013) shows that the size-dependent elastic properties of prion amyloid fibrils provide insight into the critical size of the fibril that exhibits the high infectivity. These observations suggest the necessity of measuring the nanomechanical properties of amyloid fibrils for understanding their biological functions. In addition, the insight into the nanomechanical properties of amyloid fibrils may give rise to design principles showing how the nanomechanical properties of protein fibrils can be determined. This design principle may play a leading role in developing novel biomimetic materials whose mechanical properties can be controlled (Solar and Buehler 2012b). For instance, Knowles *et al*. (2010) developed a biomimetic thin film based on amyloid fibrils, whose mechanical properties are comparable to those of mechanically strong protein materials such as keratin. Recently, Mezzenga and coworkers (Li *et al*. 2012) devised a biomimetic composite material composed of graphene and amyloid fibril, and showed that the nanomechanical properties of this composite material can be tuned by chemical environment (e.g., humidity). Moreover, they developed a biological composite material that is synthesized using both amyloid fibril and spider silk (Ling *et al*. 2014). These previous studies imply that the nanomechanical characterization of protein fibrils is essential for developing novel functional biomimetic materials whose properties may be controllable.

Though the nanomechanical properties of protein materials can be probed by single-molecule experiments such as AFM experiment (Muller and Dufrene 2008) and optical tweezer (Bustamante

2003), these experiments are unable to provide the detailed insight into how the molecular structure of protein material is deformed (or ruptured) by a force (Eom 2011). This restriction of single-molecule experiments can be resolved by considering the atomistic simulations such as molecular dynamics (MD) simulations, which can provide the detailed insight into the time-dependent molecular structure of protein materials in response to various stimuli including a force (Sotomayor and Schulten 2007). In particular, steered molecular dynamics (SMD) simulations have played a vital role in understanding the mechanical response of various protein domains such as muscle protein domains (Lu *et al*. 1998, Lu and Schulten 1999, Gao *et al*. 2002). In recent years, SMD simulations have been also utilized for studying the nanomechanical properties of large protein assemblies such as protein fibrils (Buehler *et al*. 2008). Specifically, SMD simulations have recently been considered to characterize the nanomechanical deformation mechanisms and properties of various protein fibrils such as spider silk crystals (Keten *et al*. 2008) and amyloid fibrils (Solar and Buehler 2014, Choi *et al*. 2015).

In this work, we have studied the role that boundary condition plays in the nanomechanical deformation behavior of amyloid fibrils and their nanomechanical properties by using SMD simulations. In particular, our work is aimed towards unveiling how the nanomechanical deformation mechanisms and properties of amyloid fibrils are affected by the way in which the fibril is deformed. It is found that the elastic modulus of amyloid fibrils is independent of boundary condition, while this boundary condition makes a critical impact on the fracture properties of amyloid fibrils. The effect of boundary condition in the fracture properties of the fibrils is attributed to the bond rupture mechanisms that are affected by the boundary condition. Our work provides insight into how the nanomechanical deformation mechanisms and properties of amyloid fibrils are determined.

2. Method

2.1 Equilibrium molecular dynamics simulation

We construct the initial structure of amyloid fibril by stacking a building block made of two β-sheet layers along the fibril axis. Here, the structure of the building block is provided in protein data bank (pdb) with the pdb code of 2KIB (Nielsen *et al*. 2009). We note that this building block consists of two β-sheet layers, where each β-sheet layer is composed of two β-strands whose sequence is given as “SNNFGAILS”. This sequence is known as an amyloidogenic core that plays a crucial role in the formation of human islet amyloid polypeptide (hIAPP) fibrils (Hoppener *et al*. 2000). The atomistic structure of amyloid fibril was visualized using visual molecular dynamics (VMD) package (Humphrey *et al*. 1996). Once the initial structure of the fibril is constructed, we performed energy minimization process using conjugate gradient method, and then equilibrium MD simulation was conducted under NPT ensemble at room temperature in ambient condition. Here, MD simulation was implemented based on NAMD package (Phillips *et al*. 2005) along with CHARMM27 force field (MacKerell *et al*. 1998). The equilibrium MD simulation was conducted until the root-mean-square distance (RMSD) of the fibril reaches a steady-state value.

2.2 Steered molecular dynamics simulation

In order to study the nanomechanical behavior and properties of amyloid fibrils, we consider

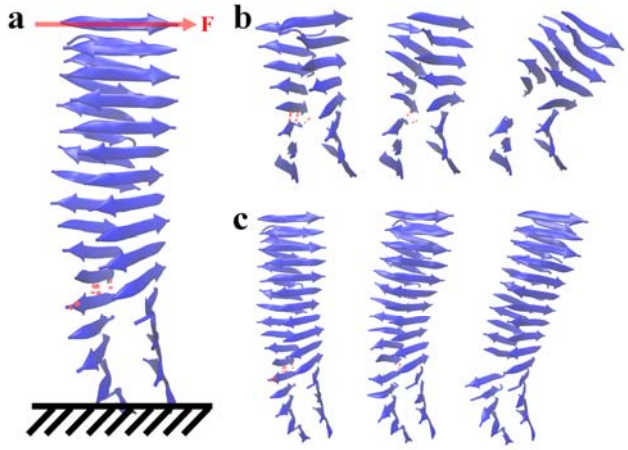

Fig. 1 Mechanical deformation mechanisms of amyloid fibrils: (a) Cantilevered boundary condition of amyloid fibril deformed by a mechanical pulling is shown. (b) Deformation mechanisms of amyloid fibril with its length of 3.41 nm are presented. (c) Deformation behaviors of amyloid fibrils with its length of 8.28 nm are shown

SMD simulations that allow for the nanomechanical deformation of the fibril. In particular, in order to mechanically pull the fibril, we connect a harmonic spring, which mimics a force probe such as AFM tip, to a specific atom of the fibril. This specific atom is gradually pulled via a harmonic spring (with its force constant of K = 10 kcal·mol^{-1}·Å^{-2}), which is moved with a constant velocity v. It is straightforward to calculate the displacement of the fibril as a function of time based on the time-dependent MD trajectories of atoms comprising the fibril, while the force to pull the fibril can be measured from Hooke's law such as $F(t)=K|R(t)–vt|$, where $R(t)$ is a distance that the pulled β strand travels. Based on the force-displacement curve of amyloid fibril, its stiffness can be extracted by measuring the slope of the linear region of the force-displacement curve for the fibril.

3. Results and discussion

3.1 Nanomechanical behavior of amyloid fibrils

In order to probe the nanomechanical deformation behavior of an amyloid fibril, we utilize SMD simulations that allow for mechanical pulling of the fibril. Here, we consider a cantilevered boundary condition, that is, one end of the fibril is fixed while the other end is mechanically pulled in a lateral direction, otherwise specified. We note that our recent SMD simulations (Choi *et al.* 2015) take into account the double-clamping boundary condition, where both ends of the fibril are fixed while the middle layer of the fibril is mechanically extended. In this work, with cantilevered boundary condition, the amyloid fibril is deformed based on the pulling speed of v=0.005 Å·ps^{-1}. The direction of pulling is parallel to the end-to-end distance of a β strand in the top layer of the fibril (Fig. 1a). It is shown that regardless of the fibril length, the deformation of the fibril

resembles the bending-like deformation (Fig. 1b and c). It is strikingly different from the case of double-clamping boundary condition as reported in our recent study (Choi *et al*. 2015), which shows that the deformation behavior of a short fibril is depicted as a shear deformation, whereas the bending deformation becomes dominant for a long fibril. This suggests the important role of boundary condition in the deformation behavior of amyloid fibrils (for details, see below).

Based on SMD simulations on the mechanical deformation of cantilevered amyloid fibril, we obtain the force-displacement curves of the fibrils (Fig. 2). These curves help us understand the nanomechanical deformation behaviors of amyloid fibrils. The force-displacement curves of amyloid fibrils, which were deformed based on double-clamping boundary condition, can be found in our recent study (Choi *et al*. 2015). It is shown that the boundary condition plays a significant role in the nanomechanical deformation behavior of amyloid fibrils. In particular, for a short amyloid fibril (with its length of L=3.41 nm), a force curve obtained from cantilevered boundary condition is different from that acquired based on double-clamping boundary condition. Specifically, when a short fibril (i.e., L=3.41 nm) is deformed based on double-clamping boundary condition, the nanomechanical response of the fibril is well fitted to linear elasticity until the displacement approaches ~0.4 nm, at which a significant force drop is observed. This force drop is due to breakage of hydrogen bonds that sustain the fibril structure. It is implied that the nanomechanical response of the short fibril is well dictated by linear elasticity with all-or-none fashion of bond rupture mechanism that occurs at a critical displacement (i.e., ~0.4 nm), which was well described in our recent study (Choi *et al*. 2015). On the other hand, when the short fibril is deformed based on cantilevered boundary condition, the linear elasticity can be employed for explaining the deformation of the short fibril as long as its displacement is <0.2 nm. Once the displacement approaches 0.2 nm, as the displacement gradually increases, so does the force that the fibril exerts. This implies that the bond rupture mechanism for the case of cantilevered boundary condition is different from that of double-clamped boundary condition. Moreover, the

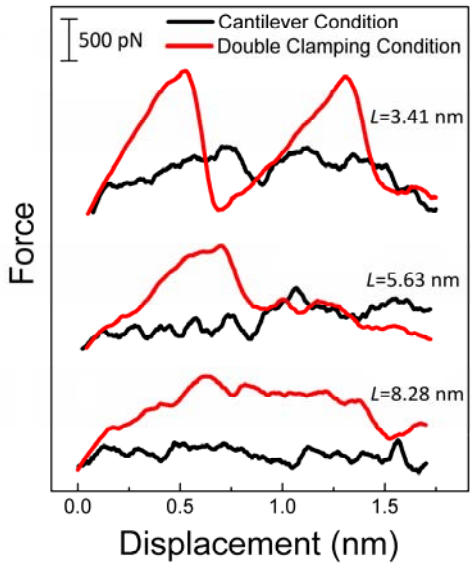

Fig. 2 Force-displacement curves of amyloid fibrils as a function of their length and boundary conditions

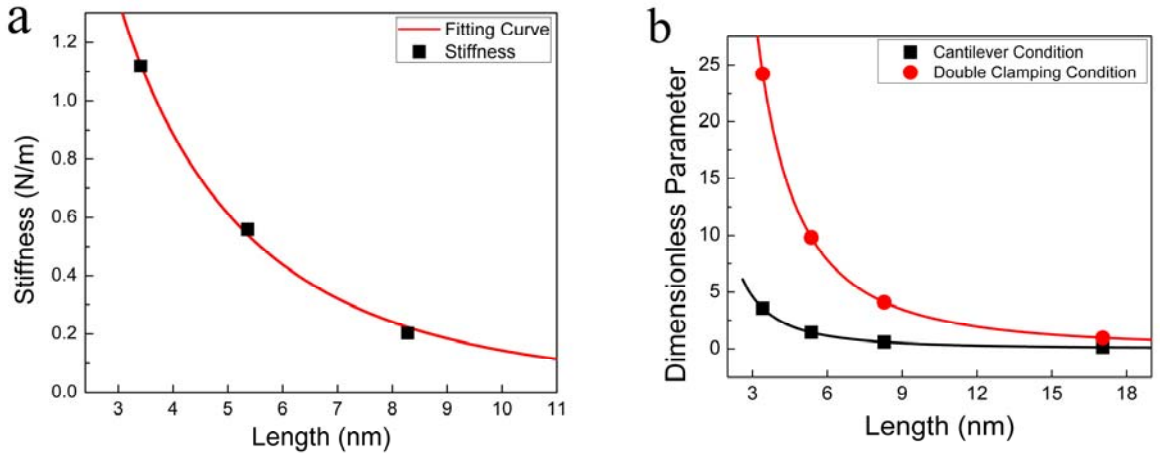

Fig. 3 Elastic properties of amyloid fibrils: (a) Elastic stiffness of amyloid fibrils, which are pulled based on cantilevered boundary condition, is shown as a function of their length scales. Solid line indicates the theoretical prediction from Timoshenko beam model, while dots represent the results obtained from SMD simulations. (b) Dimensionless parameter, χ, which quantifies how the shear deformation contributes to the elastic deformation of amyloid fibrils, is shown as a function of their length scales. The dimensionless parameter is critically dependent on the boundary condition. Solid line represents the theoretical prediction from Timoshenko beam model, whereas dots indicate the SMD simulation results

maximum force (referred to as "rupture force"), which the fibril can exert, depends on the boundary condition. Specifically, the rupture force of the fibril deformed based on double-clamping boundary condition is larger than that based on cantilevered boundary condition (for details, see Section 3.3). In addition, for an amyloid fibril with its length of L=5.63 nm, we can observe a single large force peak when the fibril is deformed based on double-clamping boundary condition until the displacement of u=~0.7 nm. However, for the cantilevered fibril that is deformed until the displacement of u=~0.7 nm, there are several force peaks that correspond to the rupture events of hydrogen bonds sustaining the fibril structure. This suggests that, for a doubly-clamped fibril, the significant rupture of hydrogen bonds is unlikely to occur until the fibril is deformed with a displacement up to u=~0.7 nm, while there are several events of hydrogen bond ruptures for the cantilevered fibril that is deformed until the displacement of u=~0.7 nm. This highlights the important role of boundary condition on the nanomechanical deformation behaviors of amyloid fibrils. Furthermore, as already reported in our recent study (Choi *et al*. 2015), the nanomechanical behaviors of amyloid fibrils are critically dependent on their length scales such that the rupture force of the fibril increases as the fibril length decreases.

3.2 Elastic properties of amyloid fibrils

Based on the force-displacement curves of amyloid fibrils (e.g., Fig. 2), we estimated their elastic stiffness, which is defined as the slope of the linear region of the force-displacement curve, i.e., $k=dF/du|_0$. Fig. 3(a) shows the elastic stiffness of amyloid fibrils with respect to their length scales. It is shown that the stiffness of amyloid fibril is increased as the fibril length decreases, which is consistent with our recent SMD simulations (Choi *et al*. 2015) that consider the doubly-clamped amyloid fibrils. However, the stiffness of the cantilevered fibril is smaller than that of

doubly-clamped fibril (Fig. 3a). For instance, for an amyloid fibril with L=3.41 nm, its stiffness is measured as k=~1.2 N/m for cantilevered boundary condition, while the stiffness is estimated as k=~3.8 N/m for double-clamping boundary condition. This clearly shows the effect of boundary conditions in the measured elastic stiffness of amyloid fibrils.

The length-dependent elastic stiffness of amyloid fibrils can be understood by considering Timoshenko beam model (Gere 2003), which takes into account not only the bending deformation of a one-dimensional structure but also its shear deformation. As already described in previous studies (Pampaloni *et al*. 2006, Keten *et al*. 2010, Xu *et al*. 2010, Yoon *et al*. 2011, Choi *et al*. 2015), the length-dependent elastic stiffness of protein fibrils is attributed to the length-dependent competition between bending and shear deformation modes. Timoshenko beam model provides the length-dependent elastic stiffness of amyloid fibril in the form of

$$k(L) = \frac{D}{L^3}\left(1 + \alpha \frac{\beta D}{G_S A L^2}\right)^{-1} \tag{1}$$

where k, L, D, G_S, and A represent the elastic stiffness, length, bending rigidity, shear modulus, and cross-sectional area of an amyloid fibril, respectively, and α is a boundary condition-dependent constant, and β is a constant that depends on the geometry of an amyloid fibril. As shown in Fig. 3a, the length-dependent elastic stiffness of amyloid fibrils is well dictated by Timoshenko beam model depicted in Eq. (1). We found the bending rigidity and shear modulus of amyloid fibrils to be measured as D=6.78×10^{-26} N·m^2 and G_S=2.28 GPa, respectively. The bending rigidity of amyloid fibrils measured based on cantilevered boundary condition is comparable to that (i.e., D=7.73×10^{-26} N·m^2) measured using double-clamping boundary condition (Choi *et al*. 2015). This suggests that the bending rigidity of amyloid fibrils is independent of boundary conditions. Moreover, the bending rigidity of hIAPP amyloid fibrils measured in this work or our recent work (Choi *et al*. 2015) is comparable to that (i.e., D=~8×10^{-26} N·m^2) computed from coarse-grained normal mode analysis based on elastic network model (Yoon *et al*. 2011). This observation elucidates that the bending rigidity of protein fibril is an intrinsic property that is independent of boundary condition as well as measuring methods, and that this intrinsic property is purely determined from the molecular structure of the fibril as reported in our recent study (Eom 2011).

In order to understand the competition between shear and bending deformation modes during the nanomechanical deformation of an amyloid fibril, we introduce a dimensionless parameter χ defined as (Yoon *et al*. 2011)

$$\chi = \alpha \frac{\beta D}{G_S A L^2} \tag{2}$$

Here, χ is a dimensionless quantity showing how the shear deformation mode contributes to the elastic deformation of an amyloid fibril. In particular, if χ is much larger than 1, then the shear deformation mode plays a leading role in the elastic deformation of an amyloid fibril. Fig. 3(b) shows the dimensionless parameter χ as a function of the fibril length. It is shown that the shear deformation dominates the elastic deformation of a very short amyloid fibril (i.e., L=3.41 nm), while the elastic deformation of a long fibril (i.e., L>~10 nm) is mostly contributed by the bending deformation. More interestingly, we found that the contribution of shear deformation to the elastic deformation of a short amyloid fibril (i.e., L=3.41 nm) is critically dependent on the boundary condition. In particular, the contribution of shear deformation to the elastic deformation of a short

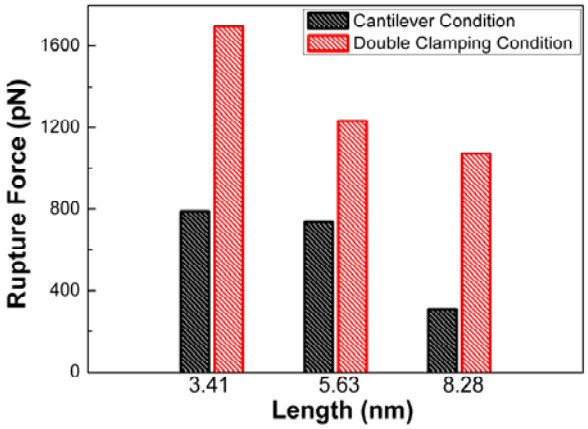

Fig. 4 Fracture properties of amyloid fibrils: The rupture force of amyloid fibrils depends on their length scales as well as boundary condition

fibril, which is deformed based on double-clamping boundary condition, is larger by a factor of ~5 than that deformed using cantilevered boundary condition (Fig. 3b). This is consistent with Fig. 1 showing that when a short fibril (i.e., L=3.41 nm) is deformed based on cantilevered boundary condition, the shear deformation does not take a leading role in its elastic deformation.

3.3 Fracture properties of amyloid fibrils

Fig. 4 shows the rupture force of amyloid fibrils as a function of their length scales. It is shown that the decrease of the fibril length increases the rupture force, which indicates that the mechanical strength of amyloid protein materials is determined from their size. However, unlike the results of our recent SMD simulations (Choi *et al*. 2015), the rupture force of the cantilevered fibril with its length of L=3.41 nm is comparable to that with L=5.63 nm. More remarkably, the rupture force of the fibril with its length of L=3.41 nm measured based on cantilevered boundary condition is smaller by a factor of ~2 than that estimated based on double-clamping boundary condition (Fig. 4). For an amyloid fibril with its length of L=8.28 nm, the rupture force measured using double-clamping boundary condition is larger by a factor of ~3 than that estimated based on cantilevered boundary condition (Fig. 4). This observation demonstrates the important role that boundary condition plays in the mechanical strength of amyloid fibrils, which implies the effect of boundary condition in the bond rupture mechanisms of the fibrils.

To understand how the boundary condition affects the mechanical strength of amyloid fibrils, we measure the fraction of hydrogen bonds that are fractured when the fibril is deformed at a critical displacement, where a maximum force peak (i.e., rupture force) appears in the force-displacement curve. Except a short fibril (i.e., L=3.41 nm), the fraction of hydrogen bonds, which were ruptured during the deformation, is critically reduced for the cantilevered boundary condition (Fig. 5). For a long amyloid fibril, though the hydrogen bonds are likely to be ruptured one-by-one (Choi *et al*. 2015), the total fraction of ruptured hydrogen bonds during the deformation of the fibril is critically dependent on the boundary condition. For instance, in the case of a fibril with its

length of L=8.28 nm, the total fraction of fractured hydrogen bonds for the fibril, which is deformed based on cantilevered boundary condition, is measured as ~1 %. On the other hand, for the fibril with L=8.28 nm, the fraction of ruptured hydrogen bonds in a case of double-clamping boundary condition is estimated as ~4%. However, for a short fibril with its length of L=3.41 nm, the total fraction of fractured hydrogen bonds during the deformation is independent of boundary conditions. In particular, for the short fibril, the total fraction of broken hydrogen bonds in a case of cantilevered boundary condition is evaluated as ~9%, while it is estimated as ~11% for the double-clamping boundary condition. Despite the minor difference between total fractions of ruptured hydrogen bonds for two different boundary conditions, the difference between rupture forces for such boundary conditions is very large as much as ~800 pN. This huge difference between rupture forces for two different boundary conditions may be attributed to the bond rupture mechanisms (i.e., deformation mechanisms) rather than the total number of fractured hydrogen bonds. As shown in Fig. 1(a), even for a short fibril with L=3.41 nm, the deformation of cantilevered fibril is not perfectly shear-like deformation, while the elastic deformation of the short fibril that is doubly-clamped is mostly contributed by perfectly shear-like deformation. In other words, for the short fibril deformed based on double-clamping boundary condition, the perfectly shear-like deformation implies that hydrogen bonds in parallel are likely to be ruptured collectively when the force acting on the fibril reaches the rupture force (Choi *et al*. 2015). This is consistent with our finding in Fig. 2 showing a single large force peak found for the short fibril, which is deformed (until the displacement of u=~4 nm) based on double-clamping boundary condition. However, for the short fibril pulled based on cantilevered boundary condition, we observe several force drops that correspond to several events of hydrogen bond ruptures. This observation indicates that, for a cantilevered short fibril, the hydrogen bonds sustaining the fibril structure are unlikely to be ruptured collectively. In summary, the fracture properties of amyloid fibrils are determined from not only the fraction of hydrogen bonds fractured until the rupture force, but also the deformation mechanisms that are related to the bond rupture mechanisms.

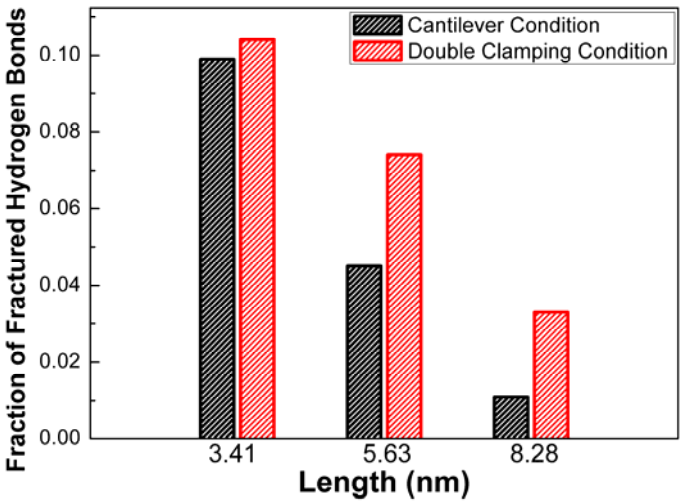

Fig. 5 Fraction of hydrogen bonds that are ruptured during the deformation of an amyloid fibril until the critical displacement, at which the rupture force appears: The number of hydrogen bonds, which were broken at the rupture force, depends on the fibril length as well as boundary condition

4. Conclusions

In this work, we have studied how the nanomechanical deformation behaviors and properties of amyloid fibrils are determined. It is shown that the length scales of amyloid fibrils determine their nanomechanical deformation behaviors and properties, and that the length-dependent elastic properties of amyloid fibrils are well dictated by Timoshenko beam model, which implies the critical role that the competition between shear and bending deformation modes plays in the elastic deformation mechanisms of the fibrils. More importantly, the elastic properties (i.e., bending rigidity D and shear modulus G_S) of amyloid fibrils are intrinsic properties that are independent of boundary conditions. However, the fracture properties of amyloid fibrils are critically dependent on the boundary conditions. This dependence of fracture properties on the boundary condition is due to the important role of boundary condition in the deformation and bond rupture mechanisms of amyloid fibrils. Our work may provide insight into how the remarkable nanomechanical properties and anomalous deformation mechanisms of amyloid fibrils are determined, which gives rise to design principles showing how the properties of protein fibrils can be achieved.

Acknowledgments

This work was supported by the National Research Foundation of Korea (NRF) under Grant No. 2015R1A2A2A04002453, SKKU Faculty Research Fund, and the National Institute of Supercomputing and Network in the Korea Institute of Science and Technology Information (KISTI) under Grant No. KSC-2015-C3-031.

References

Buehler, M.J., Keten, S. and Ackbarow, T. (2008), "Theoretical and computational hierarchical nanomechanics of protein materials: Deformation and fracture", *Prog. Mater. Sci.*, **53**(8), 1101-1241.

Bustamante, C., Bryant, Z. and Smith, S.B. (2003), "Ten years of tension: Single-molecule DNA mechanics", *Nature*, **421**(6921), 423-427.

Cherny, I. and Gazit, E. (2008), "Amyloids: Not only pathological agents but also ordered nanomaterials", *Angew. Chem. Int. Ed.*, **47**(22), 4062-4069.

Choi, B., Yoon, G., Lee, S.W. and Eom, K. (2015), "Mechanical deformation mechanisms and properties of amyloid fibrils", *Phys. Chem. Chem. Phys.*, **17**(2), 1379-1389.

Engel, M.F.M., Khemtemourian, L., Kleijer, C.C., Meeldijk, H.J.D., Jacobs, J., Verkleij, A.J., de Kruijff, B., Killian, J.A. and Hoppener, J.W.M. (2008), "Membrane damage by human islet amyloid polypeptide through fibril growth at the membrane", *Proc. Natl. Acad. Sci. USA.*, **105**(16), 6033-6038.

Eom, K. (2011), *Simulations in Nanobiotechnology*, CRC Press, Boca Raton, FL, USA.

Eom, K., Li, P.C., Makarov, D.E. and Rodin, G.J. (2003), "Relationship between the mechanical properties and topology of cross-linked polymer molecules: Parallel strands maximize the strength of model polymers and protein domains", *J. Phys. Chem. B.*, **107**(34), 8730-8733.

Eom, K., Makarov, D.E. and Rodin, G.J. (2005), "Theoretical studies of the kinetics of mechanical unfolding of cross-linked polymer chains and their implications for single-molecule pulling experiments", *Phys. Rev. E.*, **71**(2), 021904.

Fitzpatrick, A.W.P., Park, S.T. and Zewail, A.H. (2013), "Exceptional rigidity and biomechanics of amyloid revealed by 4D electron microscopy", *Proc. Natl. Acad. Sci. U.S.A.*, **110**(27), 10976-10981.

Gao, M., Wilmanns, M. and Schulten K. (2002), "Steered molecular dynamics studies of titin I1 domain

unfolding", *Biophys. J.*, **83**(6), 3435-3445.
Gere, J.M. (2003), *Mechanics of Materials*, (6th Edition), Thomson Learning, Belmont, CA, USA.
Gosline, J., Guerette, P., Ortlepp, C. and Savage, K. (1999), "The mechanical design of spider silks: From fibroin sequence to mechanical function", *J. Exp. Biol.*, **202**(23), 3295-3303.
Hamley, I.W. (2012), "The amyloid beta peptide: A chemist's perspective role in Alzheimer's and Fibrillization", *Chem. Rev.*, **112**(10), 5147-5192.
Hoppener, J.W.M., Ahren, B. and Lips, C.J.M. (2000), "Islet amyloid and type 2 diabetes mellitus", *New England J. Med.*, **343**(6), 411-419.
Humphrey, W., Dalke, A. and Schulten, K. (1996), "VMD: Visual molecular dynamics", *J. Mol. Graph.*, **14**(1), 33-38.
Keten, S., Xu, Z., Ihle, B. and Buehler, M.J. (2010), "Nanoconfinement controls stiffness, strength, and mechanical toughness of β-sheet crystals in slik", *Nat. Mater.*, **9**(4), 359-367.
Knowles, T.P., Fitzpatrick, A.W., Meehan, S., Mott, H.R., Vendruscolo, M., Dobson, C.M. and Welland, M.E. (2007), "Role of intermolecular forces in defining material properties of protein nanofibrils", *Science*, **318**(5858), 1900-1903.
Knowles, T.P.J. and Buehler, M.J. (2011), "Nanomechanics of functional and pathological amyloid materials", *Nat. Nanotech.*, **6**(8), 469-479.
Knowles, T.P.J., Oppenheim, T.W., Buell, A.K., Chirgadze, D.Y. and Welland, M.E. (2010), "Nanostructured films from hierarchical self-assembly of amyloidogenic proteins", *Nat. Nanotech.*, **5**(3), 204-207.
Li, C., Adamcik, J. and Mezzenga, R. (2012), "Biodegradable nanocomposites of amyloid fibrils and graphene with shape-memory and enzyme-sensing properties", *Nat. Nanotech.*, **7**(7), 421-427.
Ling, S., Li, C., Adamcik, J., Shao, Z., Chen, X. and Mezzenga, R. (2014), "Modulating materials by orthogonally oriented β-strands: Composites of amyloid and silk fibroin fibrils", *Adv. Mater.*, **26**(26), 4569-4574.
Lu, H.B., Isralewitz, B., Krammer, A., Vogel, V. and Schulten, K. (1998), "Unfolding of titin immunoglobulin domains by steered molecular dynamics simulation", *Biophys. J.*, **75**(2), 662-671.
Lu, H. and Schulten, K. (1999), "Steered molecular dynamics simulations of force-induced protein domain unfolding", *Proteins: Struct. Funct. Bioinfo.*, **35**(4), 453-463.
MacKerell, A.D., Bashford, D., Bellott, M., Dunbrack, R.L., Evanseck, J.D., Field, M.J., Fischer, S., Gao, J., Guo, H., Ha, S., Joseph-McCarthy, D., Kuchnir, L., Kuczera, K., Lau, F.T.K., Mattos, C., Michnick, S., Ngo, T., Nguyen, D.T., Prodhom, B., Reiher, W.E., Roux, B., Schlenkrich, M., Smith, J.C., Stote, R., Straub, J., Watanabe, M., Wiorkiewicz-Kuczera, J., Yin, D. and Karplus, M. (1998), "All-atom empirical potential for molecular modeling and dynamics studies of proteins", *J. Phys. Chem. B.*, **102**(18), 3586-3616.
Muller, D.J. and Dufrene, Y.F. (2008), "Atomic force microscopy as a multifunctional molecular toolbox in nanobiotechnology", *Nat. Nanotech.*, **3**(5), 261-269.
Nielsen, J.T., Bjerring, M., Jeppesen, M.D., Pedersen, R.O., Pedersen, J.M., Hein, K.L., Vosegaard, T., Skrypstrup, T., Otzen, D.E. and Nielsen, N.C. (2009), "Unique identification of supramolecular structures in amyloid firbils by solid-state NMR spectroscopy", *Angew. Chem. Int. Ed.*, **121**(12), 2152-2155.
Pampaloni, F., Lattanzi, G., Jonas, A., Surrey, T., Frey, E. and Florin, E.-L. (2006), "Thermal fluctuations of grafted microtubules provide evidence of a length-dependent persistent length", *Proc. Natl. Acad. Sci. USA*, **103**(27), 10248-10253.
Paparcone, R. and Buehler, M.J. (2011), "Failure of Aβ(1-40) amyloid fibrils under tensile loading", *Biomaterials*, **32**(13), 3367-3373.
Pepys, M.B. (2006), "Amyloidosis", *Annu. Rev. Med.*, **57**, 223-241.
Phillips, J.C., Braun, R., Wang, W., Gumbart, J., Tajkhorshid, E., Villa, E., Chipot, C., Skeel, R.D., Kale, L. and Schulten, K. (2005), "Scalable molecular dynamics with NAMD", *J. Comput. Chem.*, **26**(16), 1781-1802.
Silveira, J.R., Raymond, G.J., Hughson, A.G., Race, R.E., Sim, V.L., Hayes, S.F. and Caughey, B. (2005),

"The most infectious prion protein particles", *Nature*, **437**(7056), 257-261.
Smith, J.F., Knowles, T.P., Dobson, C.M. MacPhee, C.E. and Welland, M.E. (2006), "Characterization of the nanoscale properties of individual amyloid fibrils", *Proc. Natl. Acad. Sci. USA*, **103**(43), 15806-15811.
Solar, M. and Buehler, M.J. (2012a), "Comparative analysis of nanomechanics of protein filaments under lateral loading", *Nanoscale*, **4**(4), 1177-1183.
Solar, M.I. and Buehler, M.J. (2012b), "Composite materials: Taking a leaf from nature's book", *Nat. Nanotechnology*, **7**(7), 417-419.
Solar, M. and Buehler, M.J. (2014), "Tensile deformation and failure of amyloid and amyloid-like protein fibrils", *Nanotechnology*, **25**(10), 105703.
Sotomayor, M. and Schulten, K. (2007), "Single-molecule experiments *in vitro* and *in silico*", *Science*, **316**(5828), 1144-1148.
Straub, J.E. and Thirumalai, D. (2011), "Towards a molecular theory of early and late events in monomer to amyloid fibril formation", *Annu. Rev. Phys. Chem.*, **62**, 437-463.
Tanaka, M., Collins, S.R., Toyama, B.H. and Weissman, J.S. (2006), "The physical basis of how prion conformations determine strain phenotypes", *Nature*, **442**(7102), 585-589.
Xu, Z., Paparcone, R. and Buehler, M.J. (2010), "Alzheimer's Aβ(1-40) amyloid fibrils feature size-dependent mechanical properties", *Biophys. J.*, **98**(10), 2053-2062.
Yoon, G., Kim, Y.K., Eom, K. and Na, S. (2013), "Relationship between disease-specific structures of amyloid fibrils and their mechanical properties", *Appl. Phys. Lett.*, **102**(1), 011914.
Yoon, G., Kwak, J., Kim, J.I., Na, S. and Eom, K. (2011), "Mechanical characterization of amyloid fibrils using coarse-grained normal mode analysis", *Adv. Funct. Mater.*, **21**(18), 3454-3463.
Yoon, G., Lee, M., Kim, J.I., Na, S. and Eom, K. (2014), "Role of sequence and structural polymorphism on the mechanical properties of amyloid fibrils", *PLOS ONE*, **9**, e88502.

MC